

Design principle of multi-cluster and desynchronized states in oscillatory media via nonlinear global feedback

Yasuaki Kobayashi¹ and Hiroshi Kori²

¹Meme Media Laboratory, Hokkaido University, Sapporo 060-0813, Japan

²Division of Advanced Sciences, Ochadai Academic Production, Ochanomizu University, Tokyo 112-8610, Japan

E-mail: ¹kobayashi@nsc.es.hokudai.ac.jp, ²kori.hiroshi@ocha.ac.jp

Abstract. A theoretical framework is developed for a precise control of spatial patterns in oscillatory media using nonlinear global feedback, where a proper form of the feedback function corresponding to a specific pattern is predicted through the analysis of a phase diffusion equation with global coupling. In particular, feedback functions that generate the following spatial patterns are analytically given: i) 2-cluster states with an arbitrary population ratio, ii) equally populated multi-cluster states, and iii) a desynchronized state. Our method is demonstrated numerically by using the Brusselator model in the oscillatory regime. Experimental realization is also discussed.

PACS numbers: 82.40.Ck, 05.45.Xt, 05.45.-a

1. Introduction

Feedback control is a powerful method of regulating spatio-temporal dynamics and has been studied in a wide variety of fields including physics, chemistry, biology, and medical science [1]. For example, formation of various clustering patterns has been realized in the Belousov-Zhabotinsky reaction [2, 3] and in the catalytic CO oxidation reaction on Pt [4, 5, 6]. The catalytic CO oxidation systems have also been studied for the suppression of chemical turbulence [5, 7]. Moreover, considerable attention has been paid to feedback devices that suppress the pathological synchronization in the brain of Parkinson's disease patients [8, 9, 10, 11, 12, 13].

In many cases systems to be controlled are spatially extended, and reaction-diffusion systems provide a good model for the study of pattern controlling. Theoretical analyses based on reaction-diffusion systems have been done for the Belousov-Zhabotinsky reaction [3, 14, 15] and CO oxidation [16, 17, 18]. However, so far, only empirical control has been achieved for such spatially-extended systems, including above-mentioned pioneering experimental works [2, 3, 6]; there has been no general theory that *quantitatively* relates feedback inputs to spatial patterns.

On the other hand, for discrete oscillator systems, such a quantitative feedback control methodology has been established very recently by Kiss, Kori, Hudson, and Rusin [19, 20]. Their method is based on a phase model described by

$$\frac{d\phi_i}{dt} = \omega + \frac{K}{N} \sum_{j=1}^N \Gamma(\phi_i - \phi_j), \quad (1)$$

where ϕ_i ($0 \leq \phi_i < 2\pi$) is the phase of the oscillator i ($i = 1, \dots, N$), ω is the natural frequency, K is the coupling strength, and $\Gamma(\phi)$ is called the coupling function. Their method utilizes the following facts: the coupling function determines the entire collective behavior of the phase model, and any coupling function can be designed by applying an appropriately constructed feedback signal to a population of oscillators. Hence the population of oscillators can be steered to a desired synchronization behavior by taking the following two steps: (i) find a coupling function that results in a desired synchronization behavior in (1), and (ii) construct an appropriate feedback signal that yields the coupling function. A major advantage of their methodology is that the phase model can be constructed from experimentally measurable quantities only; detailed information on the intrinsic dynamics of the system is not necessary. Validity and robustness of their methodology have been confirmed both experimentally by using electro-chemical oscillators [19, 20] and numerically [20].

In this paper, by utilizing the above methodology by Kiss, Kori, Hudson, and Rusin, we develop a general theory for the global feedback control of spatially extended oscillatory media. Our approach is also based on a phase model. Since the existence of diffusive coupling plays a crucial role on the development of spatial patterns in oscillatory media, our phase model inevitably includes both diffusive and global coupling, in contrast to discrete oscillators. Studying such a phase model, we find coupling functions leading to the following spatial patterns characterized by the distribution of phases: (i) 2-cluster states with specified population ratios, (ii) equally populated multi-cluster states, and (iii) a desynchronized state. Moreover, we propose a new nonlinear feedback function without time delay, which is more convenient to design various coupling functions than that used in the previous work [19, 20]. We numerically demonstrate our proposed method by using a particular reaction-diffusion model and reproduce all the above three patterns with theoretically predicted feedback parameters.

This paper is organized as follows: In section 2, we present the basic idea of our control methodology for oscillatory media in detail. In section 3, we give a detailed analysis of the phase diffusion equation with special coupling functions that yield the above-mentioned three spatial patterns. Numerical demonstration of the theory by using the Brusselator is given in section 4. Experimental realization is discussed in section 5.

2. General control methodology

Our approach to the control of oscillatory media is closely related to the method recently proposed for the population of oscillators [19, 20]. Dynamics of discrete, identical limit-

cycle oscillators under global feedback is described by the following nonlinear dynamical equations:

$$\frac{d\mathbf{u}_i}{dt} = \mathbf{F}(\mathbf{u}_i) + \frac{K}{N}\mathbf{e} \sum_{j=1}^N h(\mathbf{u}_j), \quad (2)$$

where \mathbf{u}_i is the state vector of the i^{th} oscillator ($i = 1, \dots, N$), \mathbf{F} is a nonlinear function describing a limit cycle oscillation, K is the coupling strength, $h(\mathbf{u}_i)$ represents the feedback, and \mathbf{e} is a unit vector with only one nonzero component: we have assumed that the feedback is additively applied to the system.

When the coupling is weak, by treating the second term as a small perturbation the system is reduced to the phase model (1) [21]. In this phase description (1), synchronization behavior depends solely on the coupling function $\Gamma(\phi)$, and therefore one can control the synchronization behavior of the system if the coupling function is freely given. It has been shown [19, 20] that this can be done by applying a properly designed external feedback signal $h(\mathbf{u}_i)$ to the oscillators system. This method relies on the fact that the coupling function is the convolution of the feedback h and the phase response function $Z(\phi)$, which characterizes the sensitivity of the phase to a weak external perturbation (see Appendix A).

Since oscillatory media can be regarded as a population of oscillators that are diffusively connected, we argue that the same method works for shaping the coupling function in the phase description of oscillatory media. Consider a d -dimensional reaction-diffusion system with a global coupling:

$$\partial_t \mathbf{u} = \mathbf{F}(\mathbf{u}) + \hat{D} \nabla^2 \mathbf{u} + \frac{K}{S} \mathbf{e} \int h(\mathbf{u}) d\mathbf{x}, \quad (3)$$

where $\mathbf{u}(\mathbf{x}, t)$ is the state vector, \hat{D} denotes the diffusion matrix, $\mathbf{F}(\mathbf{u})$ is a reaction term that generates a limit cycle oscillation with the frequency ω , K is the coupling strength, \mathbf{e} is the same as above, and $h(\mathbf{u})$ represents the feedback integrated over the entire space S . We assume that the system is Benjamin-Feir stable, *i.e.*, the system undergoes spatially uniform oscillation when $K = 0$ (external control is absent). Following the standard procedure (see Appendix A), we obtain

$$\partial_t \phi(\mathbf{x}, t) = \omega + \alpha \nabla^2 \phi + \beta (\nabla \phi)^2 + \frac{K}{S} \int \Gamma(\phi(\mathbf{x}) - \phi(\mathbf{x}')) d\mathbf{x}', \quad (4)$$

where $\phi(\mathbf{x}, t)$ is the phase of local oscillation; α , and β are constants determined by the property of the oscillatory medium. As in the case of discrete oscillators, the coupling function $\Gamma(\phi)$ can be arbitrarily shaped by properly designing the feedback signal h .

For discrete oscillators, n -cluster states can be generated from the coupling function that contains n^{th} harmonics [22]. Even in the case of oscillatory media, the coupling function is expected to work in the same way to stabilize the clustering pattern. A distinct problem here, however, is that the spatial patterns are not solely determined from the global coupling but from the interplay between the diffusive coupling and the global coupling, which makes the analysis much more complicated. For example,

when clustering pattern forms, interfaces appear between the clusters due to the diffusive coupling. Then controlling of the interface motion is required to obtain desired clustering patterns.

Hence we take the following strategy. We start from a coupling function with which discrete oscillators described by equation (1) exhibit clustering or desynchronization. We then study the phase diffusion equation (4) with this coupling function to find resulting spatial patterns. Once the relation between the pattern and the coupling function is obtained, the corresponding feedback function can be found by following the same procedure as the discrete oscillators case. The key to carrying out this strategy is to find proper coupling functions that allows for analytical treatment of the phase equation. Although analytical treatment is easy for a simple coupling function as $\Gamma(\phi) = \sin(\phi + \theta)$ with a parameter θ [1], only poor spatial patterns appear with such a coupling function; higher harmonics in the coupling function are responsible for the formation of complex spatial patterns, including phase clustering behavior. In the next section we propose such analytically tractable coupling functions that produces clustering states and the desynchronized state.

3. Analysis of the phase model

In this section, we study a one-dimensional phase diffusion equation with a global coupling (4). Here we propose coupling functions that yield interesting spatial patterns; We are especially interested in two cluster states with specified population ratios, equally populated multi-cluster states, and the desynchronized state.

3.1. 2-cluster states: numerical investigation

Here we focus on the 2-cluster states with an arbitrary population ratio. In particular, we look for well-defined 2-clusters, with the phases maximally separated by π .

Discrete oscillators are known to form various clustering states, the behavior entirely governed by the form of the coupling function [22]. In special, the following coupling function yields 2-cluster states with the two phase difference equal to π :

$$\Gamma(\phi) = \sin \phi - \gamma \{\sin(2\phi + \theta) - \sin \theta\}, \quad (5)$$

where γ and θ are parameters (see Appendix B). Equation (1) with this coupling function has a family of 2-cluster solution with different population ratios of the two clusters, which are stable for some range of population ratios. Thus, starting from a random initial condition the system converges to a 2-cluster state with its population ratio determined from the initial condition.

Using this coupling function, we numerically investigate the phase diffusion equation (4) in one dimension with the system size $S = L$, taking θ as a control parameter and $\gamma = 0.3$. This equation is solved with the flux-free boundary condition by using the second-order Euler scheme, with spatial and time interval being set to $\Delta x = 0.1$ and $\Delta t = 0.01$, respectively. We set $L = 100$, $K = 0.1$, $\alpha = 0.384 \times 10^{-2}$. We assign

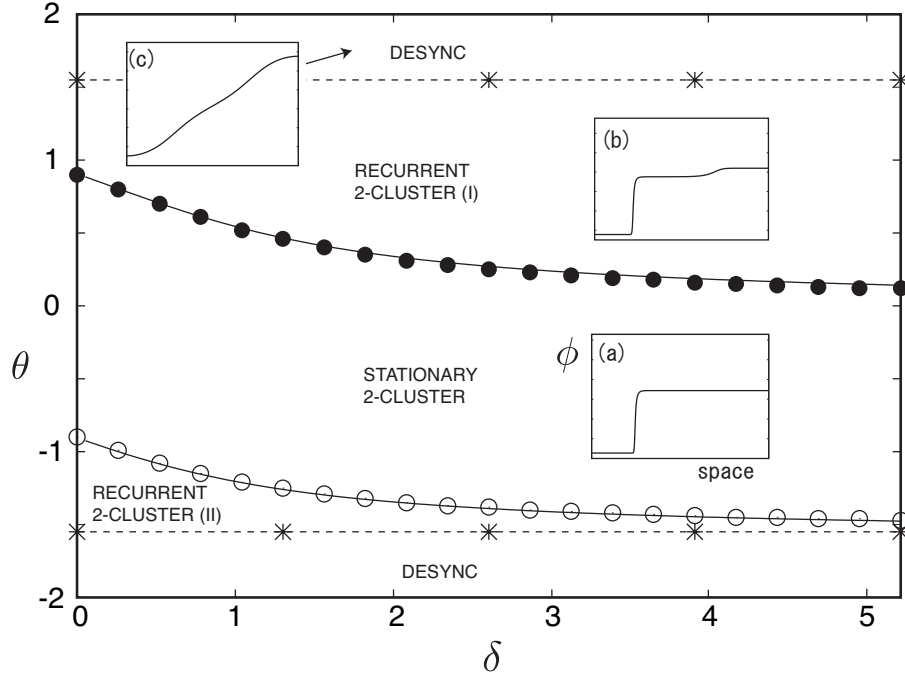


Figure 1. Phase diagram for 2-cluster states and the desynchronized state in the phase model with (5) for each $\delta = \beta/\alpha$. The points are numerical data, and the lines are given analytically. Recurrent 2-cluster has two ways of destabilization: the phase-advanced cluster becomes unstable (I), or the phase-retarded cluster becomes unstable (II). Inset figures are phase profiles with $\delta = 2.83$ and (a) $\theta = 0.23$, (b) $\theta = 0.28$, (c) $\theta = 1.58$. In (b) the pattern is not stationary; here a snapshot of budding a new cluster is shown.

several values to β to make a phase diagram below. Otherwise we set $\beta = 1.089 \times 10^{-2}$. This special choice of α and β is for later comparison to the Brusselator model.

Figure 1 shows the phase diagram obtained by varying θ for each $\delta \equiv \beta/\alpha$ with several values of β and fixed α . As expected, there exists a finite range of stationary 2-cluster states. Note that, as opposed to discrete oscillators, here the population ratio between the two clusters is uniquely determined for fixed δ and θ . Increase (decrease) in θ widens the phase-advanced (retarded) region. At some critical value of θ the stationary state becomes unstable, leading to the *recurrent* 2-cluster state, where the following process occurs in a repeated way [see figure 2(a)]: After a long transient of a quasi-stationary 2-cluster state, a new cluster sprouts out of the phase-advanced (retarded) cluster. Then the two interfaces propagate and one of the clusters disappear, the system returning to the 2-cluster state. Such dynamics have been reported in CO oxidation model [16], although investigated only numerically.

To characterize the patterns, we introduce the l^{th} order parameters ($l = 1, 2, \dots$):

$$\sigma_l = \frac{1}{L} \int dx e^{-il\phi(x)}. \quad (6)$$

For 2-cluster states, $|\sigma_1|$ indicates an approximate population disparity between the two clusters, and $1 - |\sigma_2|$ the ratio of the interface width to the system size L . Note the two

different timescales in figure 2(b), each corresponding to the emergence of a new cluster and a slow drift of the interface.

As θ exceeds the threshold around $\pm\pi/2$, the recurrent 2-clusters turn into the desynchronized state [figure 1(c)], where σ_2 almost vanishes.

3.2. 2-cluster states: analytical investigation

Here we analytically investigate the 2-cluster states numerically found above. The analysis can be done by taking $L \rightarrow \infty$ limit. We derive analytical forms of σ_1 and σ_2 as functions of θ and give the stability boundaries of the stationary 2-cluster shown in figure 1. We move to a co-rotating frame so that the phase of the phase-retarded cluster is fixed to $\phi = 0$.

As we can see from the numerical result, the profile of a 2-cluster state can be decomposed into three regions: the phase-retarded cluster denoted by A ($\phi = 0$), the phase-advanced cluster denoted by B , and the interface. Also, from the numerical observation it is implied that the instability leading to the *recurrent* 2-clusters appears from the clustered region, while the interface remains stable. Hence in the analysis below we assume that the interface does not contribute to the stability. This separation of the regions becomes well-defined for large L . When the interface width is negligible compared to the system size, the two order parameters become real. In particular, in the steady state, we have $\sigma_2 = 1$, so that σ_1 is the only relevant order parameter.

Consider the dynamics of the cluster A . Contribution of the interface comes from the global coupling represented as the integral in equation (4). Since the interface width is vanishingly small, the interface region itself does not affect the dynamics. The remaining effect of the interface comes indirectly through the interface motion that varies the population ratio of the two clusters. However, since the timescale of the interface motion is $O(1/L)$, as shown below, the population ratio can be treated as constant. Thus in this limit the dynamics of the clusters is independent of the interface motion. When the interface can be negligible, equation (4) has a solution $\phi(x) = 0$ for $x \in A$ and $\phi(x) = \pi$ for $x \in B$, where the population ratio is arbitrarily given.

The stability analysis can be performed in the same way as the discrete oscillators (see Appendix B). The only difference is the contribution from the diffusive coupling, which turns out to be negligible in the large L limit. Two modes of fluctuation occurs in the 2-cluster state: inter-cluster and intra-cluster fluctuation. Inter-cluster mode is a fluctuation of the phase between the clusters, with each cluster oscillating uniformly. The eigenvalue associated with this mode is given by $\lambda_{\text{inter}} = -1 - 2\gamma \cos \theta$. Thus by choosing $|\gamma| < \frac{1}{2}$ we can keep this mode stable. On the other hand, intra-cluster mode, a fluctuation within a cluster can be unstable. The eigenvalues associated with the cluster A and B with the wavenumber k are given by $\lambda_{\text{intra}}^{(A)} = -\alpha k^2 + 2p - 1 - 2\gamma \cos \theta$ and $\lambda_{\text{intra}}^{(B)} = -\alpha k^2 + 1 - 2p - 2\gamma \cos \theta$, respectively, where p , the population ratio, is the area fraction of the cluster A and is related to σ_1 through $2p - 1 = \sigma_1$. The negative sign of k^2 -terms implies that the diffusion always works as stabilizing the inter-cluster modes;

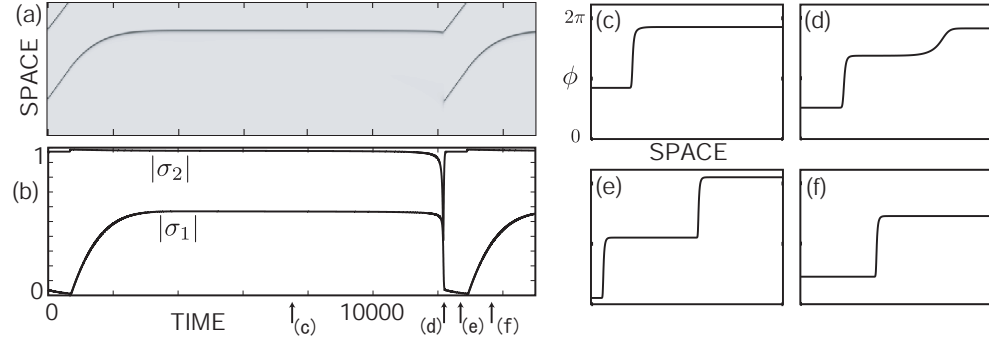


Figure 2. (a) Space-time plot of a recurrent 2-cluster for $\alpha = 0.384 \times 10^{-2}$, $\beta = 1.089 \times 10^{-2}$ and $\theta = 0.28$. Gray levels represent the spatial derivative of ϕ , with the black lines indicating the location of the interfaces. (b) Corresponding time series of the amplitude of the order parameters σ_1 and σ_2 . (c)-(f) Snapshots of the phase profile, each corresponding to the arrows in (b).

the most unstable mode is the one with the smallest (but finite) wavenumber. Taking the large L limit, this smallest wavenumber is vanishingly small, so that the k^2 -terms can be dropped from the expression of the eigenvalue.

Thus the diffusion does not affect the stability, while the stability depends on the population ratio. To obtain the analytical expression of the population ratio, let us consider the interface dynamics. The two clusters A and B are treated as the fixed boundaries of the interface. Since the inter-cluster mode is stable, the boundary conditions of the interface profile are given by $\phi(-\infty) = 0$ and $\phi(\infty) = \pi$, and σ_2 is replaced by the steady-state value, $\sigma_2 = 1$. Then equation (4) becomes

$$\partial_t \phi = \partial_x^2 \phi + \delta (\partial_x \phi)^2 + \sigma \sin \phi - \gamma (\sin(2\phi + \theta) - \sin \theta), \quad (7)$$

where we have defined $\sigma \equiv \sigma_1$ and $\delta \equiv \beta/\alpha$, and rescaled time and space as $Kt \rightarrow t$ and $\sqrt{K/\alpha} x \rightarrow x$.

Suppose that there is a traveling solution $\phi = f(x - ct)$, where the interface velocity c is written as $c = \frac{L}{2} \frac{d\sigma}{dt}$, owing to the fact that interface motion varies the population ratio. Multiplying (7) by $\partial_x f$ and integrating over the entire space yields

$$\frac{d\sigma}{dt} = -\frac{4}{L \int (\partial_x f)^2 dx} \left\{ \sigma + \frac{\delta}{2} \int (\partial_x f)^3 dx + \frac{\pi \gamma \sin \theta}{2} \right\}. \quad (8)$$

Therefore σ has a stable solution formally written as

$$\sigma = -\frac{\delta}{2} \int (\partial_x f)^3 dx - \frac{\pi \gamma \sin \theta}{2}. \quad (9)$$

From (8) it is seen that the interface slowly moves with the timescale of $O(1/L)$ toward this stable state. Thus the interface dynamics, or the time evolution of σ , is decoupled from the rest.

An explicit expression of the steady state solution of σ can be obtained through perturbation expansion. First we seek for a stationary solution of (7). When θ satisfies $\tan \theta = -\delta$, there exists an exact solution connecting $\phi(-\infty) = 0$ and $\phi(\infty) = \pi$:

$$\phi_0(x) = 2 \arctan e^{\kappa x}, \quad (10)$$

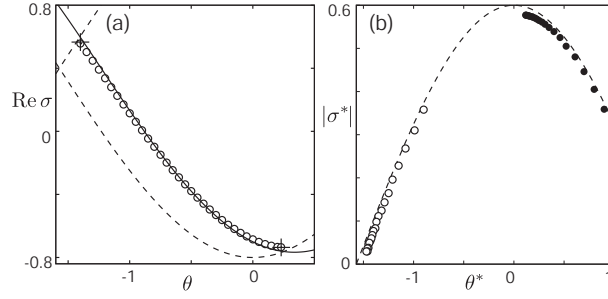


Figure 3. (a) Relation between the real part of σ and θ for $\alpha = 0.384 \times 10^{-2}$ and $\beta = 1.089 \times 10^{-2}$. The open circles are numerical data; the dotted lines represent the boundary of the existence of stationary 2-cluster states, given by (12); the solid line is given by (11); crosses at $\theta = -1.40$ and $\theta = 0.23$ are numerical data from the Brusselator model with corresponding parameters. (b) Relation between critical values of σ and θ , denoted by σ^* and θ^* . The filled and open circles correspond to the instabilities of phase-advanced and phase-retarded clusters, respectively, with different values of β . The dotted line is (12).

where $\kappa = \sqrt{2\gamma \cos \theta}$. It is easily verified from (9) that this solution satisfies $\sigma = 0$. Then perturbation expansion can be performed in terms of σ up to the first order. We obtain (see Appendix C):

$$\sigma = -\frac{2\gamma \cos \theta}{\chi(\delta)} (\delta + \tan \theta), \quad (11)$$

where $\chi(\delta) = \frac{2\delta(1+\delta^2)}{1+4\delta^2} \coth \pi\delta$.

Substituting the expression of σ into the intra-cluster eigenvalues, we obtain the stability condition of 2-cluster states. In the large L limit, the k^2 -term in the eigenvalues vanishes and the stability boundary is given by

$$\sigma \pm 2\gamma \cos \theta = 0. \quad (12)$$

Figure 3 shows the dependence of σ on θ . We have plotted only the real part of σ , while in our simulation the imaginary part is $O(K)$ and is negligible. Both equations (11) and (12) fit well with the numerical data. Moreover, substituting (11) into (12) yields

$$\tan \theta = -\delta \mp \chi(\delta), \quad (13)$$

which gives the threshold value of θ for the stability of stationary 2-cluster states. Note that the stability condition is independent of γ . The theoretical lines given by (13) are in excellent agreement with numerical data in figure 1.

Thus, within the range of parameter θ determined from (13), we can control σ as a function of θ via (11).

Now the interpretation of the recurrent 2-cluster states are given as follows: given an initial condition, the system converges to a 2-cluster state with a slowly-moving interface. When σ , varies through the interface motion, exceeds the threshold given by equation (12), the intra-cluster mode becomes unstable and one of the clusters collapses. Since the inter-cluster mode remains stable, the system returns to a 2-cluster state with reduced σ , the whole process repeated *ad infinitum*.

3.3. Desynchronized state

We give a theoretical analysis of equation (7) for the desynchronized state. The perfect desynchronized state is defined such that all the order parameters vanish. However, in practice some order parameters remain finite because of the boundary effect for flux-free boundary conditions.

Firstly, as an ideal case, let us assume the periodic boundary condition. Then the perfect desynchronized state can be given by $\phi(x) = 2\pi x/L$. Linear stability analysis for this profile shows that for each mode with the wavenumber $k_l = 2\pi l/L$ ($l \geq 1$) the corresponding eigenvalue is $\lambda_{\text{desync}}^{(l)} = \lambda_0^{(l)} - \alpha k_l^2 - 2\beta i k_l k_1$, where $\lambda_0^{(1)} = -\frac{1}{2}$, $\lambda_0^{(2)} = \gamma e^{i\theta}$, and $\lambda_0^{(l \geq 3)} = 0$. Hence the $l = 2$ mode loses the stability at $\theta = \pm \frac{\pi}{2}$ in the large L limit, which fits well with numerical data in figure 1. Note that, if the diffusive coupling is absent, only $l = 1$ and $l = 2$ modes are stable, $l \geq 3$ modes being neutral.

Since the boundary is not periodic but flux-free in the present case, the profile deviates from the linear one, as shown in figure 1(c). Accordingly, the steady state values of σ_l are shifted from zero by $O(1/L)$ (order of the width of the boundaries). Note that in the linear regime the main contribution to σ_l comes from the mode k_l . The modes $l = 1$ and $l = 2$ have the eigenvalues of order $O(1)$ as seen above, and thus σ_1 and σ_2 remains to be $O(1/L)$. On the other hand, since $l \geq 3$ modes have the eigenvalues of $O(1/L^2)$, nonlinear effects of order $O(1/L^2)$ coming from the terms such as $\sigma_1 \sigma_2$ makes $l \geq 3$ modes grow up to $O(1)$. Therefore, in order to get better desynchronized state, we need to add as many higher harmonics as possible, as demonstrated in section 4.

3.4. Multi-cluster states

The arguments of 2-cluster states can be extended to n -clusters in the following way. Consider the following coupling function:

$$\Gamma(\phi) = \sum_{m=1}^{n-1} \sin m\phi - \gamma \{\sin(n\phi + \theta) - \sin \theta\}. \quad (14)$$

This coupling function, when introduced to discrete oscillators, creates stable equally-populated n -clusters with the phases evenly separated (Appendix B). Let us find a stationary, equally populated n -cluster solution of (4) with (14). Such a solution satisfies $\sigma_m = 0$ ($m < n$) and $\sigma_n = 1$, and hence only n^{th} harmonic remains in (4). Then, by choosing θ so as to satisfy

$$\delta = -\frac{n}{2} \tan \theta, \quad (15)$$

we have a solution with each cluster separated by $\frac{2\pi}{n}$ and all the $n - 1$ interfaces having the same interface profile given by $\phi(x) = \frac{4}{n} \arctan \exp(\kappa_n x)$ with $\kappa_n = \sqrt{n\gamma \cos \theta}$. This state is stable against *inter*- and *intra*-cluster fluctuations (see Appendix B).

For the stability of the desynchronized state, the same argument as in the above $n = 2$ case holds and the stability boundary is given by $\theta = \pm \pi/2$.

4. Numerical confirmation with the Brusselator model

The above analytical expressions are used for the control of oscillatory media. As a model system of oscillatory media, we adopt the Brusselator model:

$$\frac{\partial u}{\partial t} = D_u \nabla^2 u + A - (B + 1)u + u^2 v + \frac{K}{L^d} \int h(u, v) d\mathbf{x}, \quad (16)$$

$$\frac{\partial v}{\partial t} = D_v \nabla^2 v + Bu - u^2 v. \quad (17)$$

The parameters A , B , D_u , and D_v are chosen in such a way that the system exhibits stable uniform oscillation; we set $A = 1.6$, $B = 5.0$, $D_u = 0.01$, and $D_v = 0$. The corresponding parameters in the phase model are $\alpha = 0.384 \times 10^{-2}$ and $\beta = 1.089 \times 10^{-2}$. For the precision that assures the validity of the phase description, we set $K = 0.001$ and $L = 1000$ (equivalent to $K = 0.1$ and $L = 100$ in the phase model). Note that while for convenience of numerical simulation we have set $D_v = 0$, we may also consider nonzero D_v , which simply results in the variation in the values of α and β .

As a feedback function we propose the following:

$$h(u, v) = h(\phi) = \sum_{n=0}^M k_n \cos(n\phi(u, v) - \psi_n), \quad (18)$$

where $\phi(u, v)$ is the phase of the limit cycle oscillation \ddagger , and the parameters k_n and ψ_n are the feedback intensity and the phase shift of the n^{th} feedback term, respectively. The coupling function is obtained from $h(\phi)$ and the phase response function $Z(\phi)$, which characterizes the sensitivity of the phase to a weak external perturbation (see Appendix A). By expanding $Z(\phi) = \sum_l z_l \cos(n\phi + \chi_l)$, the coupling function is written as

$$\Gamma(\phi) = \sum_{l=0}^M \frac{z_l k_l}{2} \cos(l\phi + \psi_l + \chi_l). \quad (19)$$

In principle, as long as z_l is finite, we can assign any value to l^{th} harmonics of the coupling function by choosing appropriate values for k_l and ψ_l . The advantage of using (18) is that the relation between parameters in the coupling function and the feedback parameters k_n, ψ_n is given in a simple manner. (We could also use as the feedback $h(u, v)$ a polynomial of u with multiple time delays [19, 20], but in that case the relation is represented as a nonlinear function and the parameters need to be calculated numerically.) Hence, given a coupling function, we can calculate the corresponding feedback parameters by measuring phase response function $Z(\phi)$. Table 1 shows $Z(\phi)$ and the feedback parameters corresponding to (14) for $n = 2$ and $n = 5$. In the following numerical investigation we set $\gamma = 0.3$.

\ddagger In our simulation, the phase $\phi(u, v)$ can be obtained directly from u and v in the following way: We first define the phase on the unperturbed ($K = 0$) limit cycle so that the phase evolves with a constant velocity, which can be done numerically. We then define the phase of a point (u, v) off the limit cycle by the phase of the nearest point on the limit cycle.

Table 1. Numerically obtained response function $Z(\phi) = \sum_l z_l \cos(l\phi + \chi_l)$ for the Brusselator with $A = 1.6$ and $B = 5.0$, and the feedback parameters $\{k_l\}$ and $\{\psi_l\}$ in (18) producing the coupling functions given by (14) with $n = 2$ and $n = 5$. For $l > n$, k_l and ψ_l are equal to zero.

l	z_l	χ_l	k_l ψ_l (for $n = 2$)		k_l ψ_l (for $n = 5$)	
0	0.8618	0.0	2.320 γ	$-1.570 + \theta$	2.320 γ	$-1.570 + \theta$
1	1.792	1.174	1.115	-2.745	1.115	-2.745
2	0.6390	1.410	-3.129γ	$-2.981 + \theta$	3.129	-2.981
3	0.3701	2.441			5.403	-4.012
4	0.1696	2.037			11.78	-3.608
5	0.03714	1.595			-53.84γ	$-3.165 + \theta$

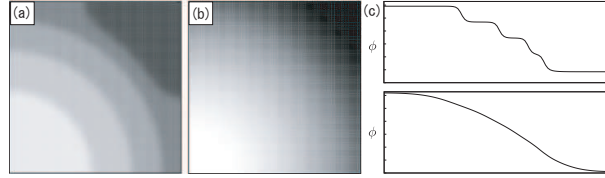


Figure 4. Two dimensional stationary pattern (uniform rotation subtracted) of the Brusselator model with global feedback containing 5 harmonics: (a) nearly equally populated 5-cluster ($\theta = -0.848$) and (b) desynchronized state ($\theta = -1.580$). (c) Section plots of (a)(top) and (b)(bottom), each from bottom left to top right.

First we study 2-cluster states in the one-dimensional case with the feedback parameters corresponding to $n = 2$. We have confirmed that, for several parameter values of θ we can observe stationary 2-clusters, recurrent 2-clusters, and desynchronized states, with the order parameter values predicted by the phase model (deviation of order $O(10^{-2})$). As an example, in figure 3(a), numerically obtained critical values of the real part of σ_1 (denoted by "+") are superimposed on the data from the phase model, which are in good agreement with the corresponding phase model, with deviations $O(10^{-2})$.

Next, we use (14) for $n = 5$ to produce the equally populated 5-cluster state and the desynchronized state in the two-dimensional case. The 5-cluster is shown in figure 4(a), the parameter θ given by (15) with $n = 5$. The order parameters are $|\sigma_5| = 0.739$ and $|\sigma_l| \sim O(10^{-2})$ for $l < 5$, indicating that the five clusters are well-defined and approximately equally populated. In figure 4(b) we have a desynchronized state with θ just below the threshold ($\theta = -1.58$), where $|\sigma_l| \sim O(10^{-3})$ for $l \leq 5$ and $O(10^{-2})$ for $l > 5$. Note that the degree of desynchronization becomes better than the one for $n = 2$ shown in section 3; we can make a better desynchronized state by adding appropriate higher harmonics.

5. Discussion: experimental realization of the theory

To apply our method to experimental systems, we need to find the constants α and β , and the response function $Z(\phi)$. Since it is generally expected that the target pattern appears in the oscillatory media (due to inhomogeneities, or by applying a manual stimulus) [21], β can be measured by using the target pattern, assuming its phase profile as $\phi(\mathbf{x}, t) = \Omega t + k|\mathbf{x}|$ (the origin is on the center of the target pattern) with the measurable quantities k and Ω : Substituting this expression into (4) with $K = 0$ we obtain $\beta = (\Omega - \omega)/k^2$. The decay rate of the local perturbation from a uniform oscillation gives α . The response function $Z(\phi)$ can be measured by perturbing the system through a global parameter, to which we also apply the global feedback. To use (18), instantaneous measurement of the phase $\phi(\mathbf{x}, t)$ at each spatial point is needed. If at least one quantity of an oscillator is observable, this can be done by, for example, constructing a delayed coordinate.

Moreover, the following things should be taken into account for experimental realization of our theory. First, feedback must be weak for the precision of the phase description. This implies that the system size should be large enough to obtain well-defined cluster states even under weak feedback: the width of the interface is $O(\sqrt{D/K})$, which must be sufficiently smaller than the linear dimension L . Also, to make a coupling function containing large enough higher harmonics with weak feedback, oscillation is better to be relaxation type: then the response function has higher harmonics with large amplitudes, so that we can keep the feedback signal weak to realize a desired coupling function [see the expression of $\Gamma(\phi)$ (19)]. Second, the emergence of phase singularity leads to the breakdown of the phase description and must be avoided.

We have checked in our preliminary numerical simulations that the multi-cluster states and the desynchronized state are robust against noise. Thus we are convinced that our proposed method works in experimental systems.

6. Concluding remarks

We have proposed a theoretical framework for designing spatial patterns in oscillatory media. When a certain pattern is found in a phase model with a specific coupling function, the same pattern can be realized in oscillatory media by applying a properly constructed nonlinear feedback. In this paper, we found analytically tractable coupling functions that enables us to quantitatively control the spatial patterns. Using these coupling functions, we investigated the phase equation with the global coupling and found the parameter regions where the following patterns stably exist: 2-cluster states with specified population ratios, equally populated multi-cluster states, and the desynchronized state. In the case of 2-clusters, we gave analytical expression of the population ratio of the two clusters as the function of a feedback parameter. We also proposed a simple form of the nonlinear feedback function to make the calculation of the feedback parameters easier. We exemplified all these results using the Brusselator

model and succeeded to reproduce the patterns predicted by the phase model. Since our method is based on the measurable quantities only, it is expected that the method is verified in a real experiment.

The desynchronized state deserves further remark. Our results show that even in oscillatory media one can drive the system into the desynchronized state, as well as in discrete oscillators [19]. Such a control is not only of medical [19, 23], but also potentially of industrial interest; for example, it would be beneficial when constant output from oscillatory catalytic reaction is desirable.

Further investigation of the phase model with other coupling functions is of great interest for controlling more complex patterns, although our method is limited to oscillatory system and cannot be applied to some typical spatial patterns such as the Turing pattern. Also, investigating the control of Benjamin-Feir unstable systems by replacing the phase diffusion equation with Kuramoto-Sivashinsky equation will be interesting both in a theoretical sense and for application.

Acknowledgments

The authors are grateful to Y. Nishiura and A. S. Mikhailov for valuable discussions.

Appendix A. Derivation of the phase model

In this Appendix we derive the phase model (4) from a reaction-diffusion system with a global feedback. The system is assumed to undergo spatially uniform oscillation when external control is absent (namely, the system is Benjamin-Feir stable [21]). Dynamical evolution of a d -dimensional oscillatory medium is described by a reaction-diffusion equation:

$$\partial_t \mathbf{u} = \mathbf{F}(\mathbf{u}; q) + \hat{D} \nabla^2 \mathbf{u}. \quad (\text{A.1})$$

Note that here we consider a general situation, where the global feedback is introduced through a global parameter q . In equation (3), and in References [19, 20], the feedback is simply applied additively. External feedback is applied to q as

$$q(t) = q_0 + Kp(t), \quad (\text{A.2})$$

where q_0 and $K > 0$ are constants. By assumption, $\partial_t \mathbf{u} = \mathbf{F}(\mathbf{u}; q_0)$ yields a limit-cycle oscillation, with its solution denoted by $\mathbf{u} = \mathbf{u}_0(t)$. The function $p(t)$ describes a global feedback signal, given by

$$p(t) = \frac{1}{S} \int h(\mathbf{u}) d\mathbf{x}, \quad (\text{A.3})$$

where $h(\mathbf{u})$ is some feedback function. The integration is taken over the entire space and S is the volume of the system. (Various functions can be considered for h . Our particular choice has been given in equation 18.)

As we have assumed, feedback intensity K is small, so that by dropping $O(K^2)$ equation (A.1) can be approximated by

$$\partial_t \mathbf{u} = \mathbf{F}(\mathbf{u}; q_0) + \hat{D} \nabla^2 \mathbf{u} + Kp(t) \mathbf{f}(\mathbf{u}), \quad (\text{A.4})$$

where $\mathbf{f}(\mathbf{u}) \equiv (\partial \mathbf{F} / \partial q)_{q=q_0}$. When \mathbf{f} is independent of \mathbf{u} , the global parameter q appears additively and the system reduces to equation (3).

When a spatial pattern emerges for small $K > 0$, the spatial variation, and thus $\nabla^2 \mathbf{u}$, is expected to be small, vanishing as $K \rightarrow 0$. Thus, in addition to the feedback term, we may treat the diffusion term as small perturbations to the limit cycle (this is the case in our simulation, where the interface width is $O(\sqrt{D/K})$), and therefore the diffusion term is the same order as the feedback). Then, following a standard method developed by Kuramoto [21], we can derive a closed description for the phase variable for our oscillatory medium. As is usually adopted, the phase $\phi(\mathbf{u})$ is defined so as to satisfy $\partial_{\mathbf{u}} \phi \cdot \mathbf{F}(\mathbf{u}; q_0) = \omega$. Substituting this relation into the identity $\partial_t \phi = \partial_{\mathbf{u}} \phi \cdot \partial_t \mathbf{u}$, we obtain

$$\partial_t \phi = \omega + \partial_{\mathbf{u}} \phi \cdot \left\{ \hat{D} \nabla^2 \mathbf{u} + Kp(t) \mathbf{f}(\mathbf{u}) \right\}. \quad (\text{A.5})$$

At the lowest order of K , we can replace \mathbf{u} with the value on the limit cycle \mathbf{u}_0 . Then the equation above is expressed only in terms of ϕ . After averaging (A.5) over one period of oscillation, we arrive at equation (4), where α , β , and $\Gamma(\phi)$ are written as

$$\alpha = \frac{1}{2\pi} \int_0^{2\pi} d\phi \tilde{\mathbf{Z}}(\phi) \hat{D} \frac{\partial \mathbf{u}}{\partial \phi}, \quad (\text{A.6})$$

$$\beta = \frac{1}{2\pi} \int_0^{2\pi} d\phi \tilde{\mathbf{Z}}(\phi) \hat{D} \frac{\partial^2 \mathbf{u}}{\partial \phi^2}, \quad (\text{A.7})$$

$$\Gamma(\phi - \phi') = \frac{1}{2\pi} \int_0^{2\pi} d\lambda Z(\phi + \lambda) h(\phi' + \lambda). \quad (\text{A.8})$$

Here, the phase response function $Z(\phi) \equiv \tilde{\mathbf{Z}}(\phi) \cdot \mathbf{f}(\phi)$, defined as the response to the global parameter q , and the “bare” response function $\tilde{\mathbf{Z}}(\phi) \equiv \partial_{\mathbf{u}} \phi|_{\mathbf{u}=\mathbf{u}_0}$, are evaluated on the unperturbed limit-cycle orbit.

Expanding $Z(\phi)$ and $h(\phi)$ as $Z(\phi) = \sum_{l=-\infty}^{\infty} z_l e^{il\phi}$ and $h(\phi) = \sum_{l=-M}^M h_l e^{il\phi}$ respectively, we obtain

$$\Gamma(\phi) = \sum_{l=-M}^M z_l h_{-l} e^{il\phi}. \quad (\text{A.9})$$

Hence the coupling function containing up to the M^{th} harmonics can be generated by determining $h(\phi)$ up to the M^{th} harmonics, as long as z_l has a finite value [19, 20].

Appendix B. 2-cluster states for the coupled oscillators

Here we show that the collection of discrete oscillators interacting through the coupling function given by (5) can exhibit 2-cluster states with their phases separated by π .

Appendix B.1. Steady-state 2-cluster solution

Consider a set of N identical oscillators with the frequency ω . The dynamics is written as

$$\dot{\phi}_i = \omega + \frac{K}{N} \sum_{j=1}^N \Gamma(\phi_i - \phi_j). \quad (\text{B.1})$$

To produce n -cluster states, it is sufficient that the coupling function contains up to the n^{th} harmonics [22]; linear stability analysis shows that the harmonics smaller than n does not contribute to the stability of n -cluster states, and the n^{th} harmonics works in a similar way to $n:1$ periodic forcing [1]. In special, to observe 2-cluster states, one needs to prepare the coupling function such that the first harmonics destabilizes the 1-cluster, *i.e.*, perfect synchronization, and the second assures the 2-cluster. Thus the coupling function for 2-cluster states can be written as

$$\Gamma(\phi) = \sin(\phi + \theta_1) - \gamma \sin(2\phi + \theta_2). \quad (\text{B.2})$$

The amplitude of the first harmonics can be absorbed into the coupling constant K . Also, for later convenience we choose the negative sign for the second harmonics.

Assume that the oscillators form a 2-cluster state, where N_A oscillators belong to the cluster A with the phase ϕ_A and $N - N_A$ to the cluster B with ϕ_B . In the phase-locking state ($\dot{\phi}_i = \Omega$ for all i), we get

$$\Omega = p\Gamma(0) + (1 - p)\Gamma(\psi), \quad (\text{B.3})$$

$$\Omega = p\Gamma(-\psi) + p\Gamma(0), \quad (\text{B.4})$$

where $\psi = \phi_A - \phi_B$, $p = N_A/N$ and $\Omega = \omega + \sin \theta_1 - \gamma \sin \theta_2$ is the frequency of the clusters. Then ψ satisfies

$$(2p - 1)\Gamma(0) + (1 - p)\Gamma(\psi) - p\Gamma(-\psi) = 0. \quad (\text{B.5})$$

When we choose $\theta_1 = 0$, (B.5) has a solution $\psi = \pi$ for any p . In special, when $|\gamma| < \frac{1}{2}$, $\psi = \pi$ is the only solution except for $\psi = 0$, the single cluster solution. If $\theta_1 \neq 0$, the phase difference is shifted from π except for $p = \frac{1}{2}$.

Appendix B.2. Linear stability analysis

We perform the linear stability analysis by expanding ϕ_j as $\phi_j = \phi_j^{(0)} + \xi_j$, where $\phi_j^{(0)} = 0$ for $j \in A$ and $\phi_j^{(0)} = \pi$ for $j \in B$.

First we consider the *inter*-cluster mode, where the fluctuation is uniform in each cluster. In this case we can write $\xi_{j \in A} = \xi_A$ and $\xi_{j \in B} = \xi_B$. The mode ξ_A obeys

$$\dot{\xi}_A = K(1 - p)\Gamma'(\pi)(\xi_A - \xi_B), \quad (\text{B.6})$$

$$\dot{\xi}_B = Kp\Gamma'(-\pi)(\xi_B - \xi_A). \quad (\text{B.7})$$

Changing the variables as $\xi_{\pm} = \xi_A \pm \xi_B$, and using $\Gamma'(\pi) = \Gamma'(-\pi) = -1 - 2\gamma \cos \theta$, we obtain

$$\dot{\xi}_+ = K(1 - 2p)(1 + 2\gamma \cos \theta)\xi_-, \quad (\text{B.8})$$

$$\dot{\xi}_- = -K(1 + 2\gamma \cos \theta)\xi_-. \quad (\text{B.9})$$

The zero mode ξ_+ represents uniform rotation along with the limit cycle. On the other hand, ξ_- corresponds to the inter-cluster mode, which is stable regardless of θ for $|\gamma| < \frac{1}{2}$.

Next we consider the *intra*-cluster mode, where the fluctuation occurs within each cluster and the spatial average of ξ within each cluster is zero. We get

$$\dot{\xi}_{j \in A} = K(2p - 1 - 2\gamma \cos \theta) \xi_{j \in A}, \quad (\text{B.10})$$

$$\dot{\xi}_{j \in B} = K(1 - 2p - 2\gamma \cos \theta) \xi_{j \in B}. \quad (\text{B.11})$$

$$(\text{B.12})$$

Thus the intra-cluster fluctuation the eigenvalues $\lambda_A = K(2p - 1 - 2\gamma \cos \theta)$ and $\lambda_B = K(1 - 2p - 2\gamma \cos \theta)$. These modes can be destabilized depending on the population ratio p . In special, when $|\theta| > \pi/2$, either λ_A or λ_B is positive for any p .

Similarly, the coupling function (14) produces n -cluster solutions $\phi_i = 2\pi l/n$ ($l = 0, \dots, n-1$) for arbitrary population ratio, as can be checked by direct substitution. Stability is studied analogously with the $n = 2$ case above, the *intra*- and *inter*-cluster eigenvalues given by

$$\lambda_{\text{inter}}^{(n)} = -K \left(\frac{n}{2} + n\gamma \cos \theta \right), \quad (\text{B.13})$$

$$\lambda_{\text{intra}}^{(n)} = -K \left(\frac{n}{2} - \frac{n^2}{2} p_m + n\gamma \cos \theta \right), \quad (\text{B.14})$$

where p_m is the fraction of the m^{th} cluster. When the clusters are equally populated, $\lambda_{\text{intra}}^{(n)} = -Kn\gamma \cos \theta$ and is stable for $|\theta| < \pi/2$. Conversely, when $|\theta| > \pi/2$ at least one of n clusters has positive $\lambda_{\text{intra}}^{(n)}$ and the n -cluster state is no longer stable.

Appendix C. Derivation of (11)

We expand the parameter θ and the profile $\phi(x)$ in terms of σ as follows:

$$\tan \theta = -\delta + \sigma \mu_1 + O(\sigma^2), \quad (\text{C.1})$$

$$\phi(x) = \phi_0(x) + \sigma \phi_1(x) + O(\sigma^2). \quad (\text{C.2})$$

Substituting these expressions into (7) yields the following linearized equation:

$$\mathcal{L}\phi_1(x) = -2\gamma \cos \theta \sin \phi_0(x) - \mu_1 \sin^2 \phi_0(x), \quad (\text{C.3})$$

where the linearized operator \mathcal{L} is given by

$$\mathcal{L} = \kappa^{-2} \partial_x^2 - \cos 2\phi_0(x) + 2\delta \sin \phi_0(x) (\kappa^{-1} \partial_x - \cos \phi_0(x)). \quad (\text{C.4})$$

The adjoint operator \mathcal{L}^\dagger is written as

$$\mathcal{L}^\dagger = \kappa^{-2} \partial_x^2 - \cos 2\phi_0(x) - 2\delta \sin \phi_0(x) (\kappa^{-1} \partial_x + 2 \cos \phi_0(x)). \quad (\text{C.5})$$

It is verified by direct calculation that \mathcal{L}^\dagger has the zero eigenfunction $\exp[2\delta \phi_0(x)] \text{sech} \kappa x$. The solvability condition reads

$$\int_{-\infty}^{\infty} dx \exp[2\delta \phi_0(x)] \text{sech} \kappa x (-2\gamma \cos \theta \sin \phi_0(x) - \mu_1 \sin^2 \phi_0(x)) = 0, \quad (\text{C.6})$$

which yields

$$\mu_1 = \frac{\delta(1 + \delta^2) \coth \pi \delta}{\gamma \cos \theta (1 + 4\delta^2)}. \quad (\text{C.7})$$

Using the relation $\tan \theta = -\delta + \sigma \mu_1$, we obtain (11).

References

- [1] A. S. Mikhailov and K. Showalter. Control of waves, patterns and turbulence in chemical systems. *Phys. Rep.*, 425:79, 2006.
- [2] Vladimir K. Vanag, Lingfa Yang, Milos Dolnik, Anatol M. Zhabotinsky, and Irving R. Epstein. Oscillatory cluster patterns in a homogeneous chemical system with global feedback. *Nature*, 406:389, 2000.
- [3] V. K. Vanag, A. M. Zhabotinsky, and I. R. Epstein. Pattern formation in the Belousov-Zhabotinsky reaction with photochemical global feedback. *J. Phys. Chem.*, 104:11566, 2000.
- [4] M. Pollmann, M. Bertram, and H. H. Rotermund. Influence of time delayed global feedback on pattern formation in oscillatory CO oxidation on Pt(110). *Chem. Phys. Lett.*, 346:123, 2001.
- [5] M. Bertram, C. Beta, M. Pollmann, A. S. Mikhailov, H. H. Rotermund, and G. Ertl. Pattern formation on the edge of chaos: Experiments with CO oxidation on a Pt(110) surface under global delayed feedback. *Phys. Rev. E*, 67:036208, 2003.
- [6] M. Kim, M. Bertram, M. Pollman, A. von Oertzen, A. S. Mikhailov, H. H. Rotermund, and G. Ertl. Controlling chemical turbulence by global delayed feedback: Pattern formation in catalytic CO oxidation on Pt(110). *Science*, 292:1357, 2001.
- [7] C. Beta, M. Bertram, A. S. Mikhailov, H. H. Rotermund, and G. Ertl. Controlling turbulence in a surface chemical reaction by time-delay autosynchronization. *Phys. Rev. E*, 67:046224, 2003.
- [8] O. V. Popovych, C. Hauptmann, and P. A. Tass. Effective desynchronization by nonlinear delayed feedback. *Phys. Rev. Lett.*, 94:164192, 2005.
- [9] C. Hauptmann, O. V. Popovych, and P. A. Tass. Delayed feedback control of synchronization in locally coupled neuronal networks. *Neurocomputing*, 65:759, 2005.
- [10] O. V. Popovych, C. Hauptmann, and P. A. Tass. Control of neuronal synchrony by nonlinear delayed feedback. *Biological Cybernetics*, 95:69, 2006.
- [11] N. Tukhlina, M. Rosenblum, A. Pikovsky, and J. Kurths. Feedback suppression of neural synchrony by vanishing stimulation. *Phys. Rev. E*, 75:011918, 2007.
- [12] M. G. Rosenblum and A. S. Pikovsky. Controlling synchronization in an ensemble of globally coupled oscillators. *Phys. Rev. Lett.*, 92:114102, 2004.
- [13] M. Rosenblum and A. Pikovsky. Delayed feedback control of collective synchrony: An approach to suppression of pathological brain rhythms. *Phys. Rev. E*, 70:041904, 2004.
- [14] L. Yang, M. Dolnik, A. M. Zhabotinsky, and I. R. Epstein. Oscillatory clusters in a model of the photosensitive Belousov-Zhabotinsky reaction system with global feedback. *Phys. Rev. E*, 62:6414, 2000.
- [15] H. G. Rotstein, N. Kopell, A. M. Zhabotinsky, and I. R. Epstein. Canard phenomenon and localization of oscillations in the Belousov-Zhabotinsky reaction with global feedback. *J. Chem. Phys.*, 119:8824, 2003.
- [16] M. Bertram and A. S. Mikhailov. Pattern formation on the edge of chaos: Mathematical modeling of co oxidation on a Pt(110) surface under global delayed feedback. *Phys. Rev. E*, 67:036207, 2003.
- [17] C. Beta and A. S. Mikhailov. Controlling spatiotemporal chaos in oscillatory reaction-diffusion system by time-delay autosynchronization. *Physica D*, 199:173, 2004.
- [18] P. Parmananda and J. L. Hudson. Controlling spatiotemporal chemical chaos using delayed feedback. *Phys. Rev. E*, 64:037201, 2001.

- [19] Istvan Z. Kiss, Craig G. Rusin, Hiroshi Kori, and John L. Hudson. “Engineering Complex Dynamical Structures: Sequential Patterns and Desynchronization”. *Science*, 316:1886, 2007.
- [20] H. Kori, C. G. Rusin, I. Z. Kiss, and J. L. Hudson. Synchronization engineering: Theoretical framework and application to dynamical clustering. *Chaos*, 18:026111, 2008.
- [21] Y. Kuramoto. *Chemical Oscillations, Waves, and Turbulence*. Springer, New York, 1984.
- [22] K. Okuda. Variety and generality of clustering in globally coupled oscillators. *Physica D*, 63:424, 1993.
- [23] William. L. Kath and Julio. M. Ottino. “Rhythm Engineering”. *Science*, 316:1857, 2007.